2012

Giant interlayer magnetoresistances and strong anisotropy in p-type Sb2Te3 single crystals

Zengji Yue
University of Wollongong, zy709@uowmail.edu.au

Xiaolin Wang
University of Wollongong, xiaolin@uow.edu.au

S X. Dou
University of Wollongong, shi@uow.edu.au

Giant interlayer magnetoresistances and strong anisotropy in p-type Sb2Te3 single crystals

Abstract

Anisotropic interlayer magneto-transport properties have been studied over a broad range of temperatures and magnetic fields in p-type Sb2Te3 single crystals. Giant interlayer magnetoresistance (MR) of up to 400% was observed, which exhibits quadratic field dependences in low fields and becomes linear at high fields without any trend towards saturation. The interlayer MR displays strong anisotropy and is attributable to the anisotropy of the Fermi surface. The observed giant anisotropic interlayer MR could find applications in p-type Sb2Te3 based magneto-electronic devices.

Keywords

crystals, type, single, p, anisotropy, strong, magnetoresistances, interlayer, giant, sb2te3

Disciplines

Engineering | Physical Sciences and Mathematics

Publication Details

Yue, Z., Wang, X. & Dou, S. (2012). Giant interlayer magnetoresistances and strong anisotropy in p-type Sb2Te3 single crystals. Integrated Ferroelectrics, 140 (1), 155-160.

Giant Interlayer Magnetoresistances and Strong Anisotropy in *p*-type Sb_2Te_3 Single Crystals

ZENGJI YUE, XIAOLIN WANG,* SHIXUE DOU

Spintronic and Electronic Materials Group, Institute for Superconducting and Electronic Materials, University of Wollongong, NSW 2522, Australia

Anisotropic interlayer magneto-transport properties have been studied over a broad range of temperatures and magnetic fields in p-type Sb_2Te_3 *single crystals. Giant interlayer magnetoresistance (MR) of up to 400% was observed, which exhibits quadratic field dependences in low fields and becomes linear at high fields without any trend towards saturation. The interlayer MR displays strong anisotropy and is attributable to the anisotropy of the Fermi surface. The observed giant anisotropic interlayer MR could find applications in p-type* Sb_2Te_3 *based magneto-electronic devices.*

Key words Giant magneto-resistance, anisotropy, Fermi surface

Corresponding author E-mail: xiaolin@uow.edu.au

1. Introduction

Topological insulators are quantum materials with an insulating bulk state and a topologically protected metallic surface state with spin and momentum helical locking and a Dirac-like band structure.[1,2] Unique and fascinating electronic properties, such as the quantum spin Hall effect, magneto-electric effects, magnetic monopoles, and elusive Majorana states, are expected from topological insulators.[3,4] Topological insulators have great potential applications in spintronics and quantum information processing, as well as magneto-electric devices with higher energy efficiency.[5,6] Up to now, the surface states in topological insulators have been mainly investigated by angle-resolved photoemission spectroscopy (ARPES), scanning tunneling microscopy (STM) and theoretical calculations.[4,7] Recently, based on band structure calculations, Bi_2Te_3, Sb_2Te_3, and Bi_2Se_3 have been identified as three-dimensional topological insulators with robust surface states comprising a single Dirac cone.[8] Shubnikov-de Haas and Aharonov–Bohm oscillations have been observed in Bi_2Se_3 and $Bi_{1-x}Sb_x$ topological insulators.[9,10,11] Low temperature linear MR was observed in Bi_2Te_3 crystal flakes and Bi_2Se_3 nano-ribbons, which was attributed to magneto-transport behavior of the gapless surface states on the surfaces of those three dimensional topological insulators.[10,12]

The bulk transport properties of topological insulators are indeed significant and interesting since the topological surface states are controlled by bulk spin-orbital coupling and closely correlated with their bulk states. To understand the macroscopic mechanisms and properties of topological surface states and to investigate the possibility of their device applications, bulk magneto-transport measurements of high-quality crystals are indispensable. Among the three dimensional topological insulators, Bi_2Te_3, Bi_2Se_3 and Sb_2Te_3, the transport study of Sb_2Te_3 is very limited. To our knowledge, there are no any reports on the interlayer magneto-transport properties of the *p*-type Sb_2Te_3 bulk single crystal samples so far. Therefore, the motivation of our work is to explore the interlayer magneto-transport properties of the *p*-type Sb_2Te_3 crystals, and we did discover very interesting results such as giant interlayer MR as high as 400% and two fold oscillation of interlayer MR in the *p*-type bulk Sb_2Te_3 single crystals. These observations are significant both for its correlation to topological surface states and potential applications in magneto-eletronic devices.

2. Experiment

2.1. Materials and Instrumentation

Layered Sb_2Te_3 has a rhombohedral structure with space group D^5_{3d} and lattice constants a = 4.34 Å and c = 30.22 Å. Very recently, $(Bi_xSb_{1-x})_2Te_3$ ternary compounds were confirmed as topological insulators with gapless Dirac-type surface states for the entire composition range by angle resolved ARPES measurements and band structure calculations.[14,15] With Bi: Sb ratio < 1:1, Sb_2Te_3 becomes *p*-type with the Fermi surface residing in the bulk valence band.[14,15] It is well-known that the *p*-type Sb_2Te_3 bulks are of particular interest and have been intensively studied because of their excellent thermoelectric performance in the vicinity of room temperature. Here, we report interlayer magneto-transport properties and angular dependent interlayer MR in *p*-type Sb_2Te_3 bulk single crystals. We observed giant and anisotropic interlayer MR in *p*-type Sb_2Te_3 single crystal samples. The observed giant, non-saturating, and highly anisotropic interlayer MR makes the Sb_2Te_3 bulk crystals useful in magneto-electric applications and is also beneficial for understanding the topological metallic states at the surface of the crystals.

2.2. Experiment Methods

The *p*-type Bi doped Sb_2Te_3 single crystals used for this study were cleaved from bulk crystals with 99.99% purity. Four-probe transport measurements were performed on a rectangular sample with dimensions of 3 × 1.15 × 1.15 mm^3 between 2 K and 300 K using a Quantum Design 14T Physical Properties Measurement System (PPMS). The resistance was obtained by applying an electric current I (typically 5000 μA) through the two outer contacts and monitoring the voltage drop V between the two inner contacts (typical spacing 1 mm), as shown in the inset of Fig. 1. The current I was applied along the C_3 axis, and the magnetic field B was applied in C_2C_3 plane. For some selected magnetic field directions, the field dependence of the interlayer MR was measured by sweeping B between 0 T and 13 T. Rotation of the sample in constant magnetic field B was used to measure the anisotropic interlayer MR.

3. Experiment Results

3.1. Resistivity

Figure 1 shows the temperature dependence of the interlayer resistivity of a *p*-type Sb_2Te_3 crystal measured in 0 T. It can be seen that the interlayer resistivity in 0 T decreases with the temperature and stays constant from 10 K down to 2 K. Such metallic R (T) curves are typical behavior for doped Sb_2Te_3 and result from the hole-type bulk carriers induced by Sb-Te anti-site defects.[16] From the Hall measurements, we determined that the bulk carrier density n is about 2×10^{19} cm^{-3}, and the bulk carrier mobility μ is 1900 cm^2/Vs, in agreement with what has been reported for typical *p*-type Sb_2Te_3 bulks.[17]

3.2. Magnetoresistance

Figure 2 displays the interlayer MR measured at several temperatures in 13 T and θ = 0°. At low magnetic fields, the interlayer MR exhibits an almost quadratic field dependence for all the temperatures, which can be fitted by MR = kB^2, with k a constant. The parabola-like B dependence of MR is likely due to the Lorentzian deflection of carriers under the perpendicular magnetic field and is a bulk-dominated effect.

The electron executes cyclotron orbits, thereby shortening the mean free path, and thus increasing the resistance. It should be noted that what is remarkable is that the pattern of curves evolves linearly in applied higher magnetic field, and the linearity is observed at all selected degrees. The interlayer MR is always positive and gradually increases as the temperatures are decreased. The maximum interlayer MR reaches up to 400%, in 13 T and 2 K. Note that the giant interlayer MR is likely to be due to the bulk states instead of the topological surface states.

3.3. Anisotropy of Magnetoresistance

Figure 3 shows the angle dependence of the interlayer MR measured in several magnetic fields at 2 K. The magnetic fields, ranging from 1 T to 13 T, were kept constant during each rotation. The observed angular dependence of the interlayer MR displays strong anisotropy and a twofold symmetry. Wide peaks appear around the perpendicular field configuration (about θ = 0º, 180º) and dips around the parallel field configuration (about θ = 90º, 270º). This suggests that the MR is most strongly pronounced in out-of-plane high fields. The interlayer MR anisotropy is most strongly pronounced in high fields at a fixed temperature. Figure 4 displays the angle-dependence of the interlayer MR measured at 13 T for various temperatures. The temperatures, ranging from 300 K to 2 K, were kept constant during each rotation. The observed angle dependence of the interlayer MR also displays anisotropic features and a twofold symmetry. The interlayer MR anisotropy and oscillations are strongly pronounced at low temperatures.

4. Result Discussions

The well-established Kohler's rule suggests that the MR of a material is a universal function of B as a result of the Lorentz force deflection of carriers. In high fields, most materials show saturating interlayer MR. Therefore, such a giant anisotropic non-saturating interlayer MR in our *p*-type Sb_2Te_3 bulk crystals is unusual. Linear quantum-MR theory was originally developed by Abrikosov based on gapless semiconductors and at the extreme quantum limit to explain the observed giant linear MR in doped silver chalcogenides.[16,18] However, it is difficult to reach the extreme quantum limit in our *p*-type Sb_2Te_3 because of high hole density. Metals that contain Fermi surfaces with open orbital in some crystallographic directions, including Cu, Ag, Au, Mg, Zn, Sn, Pb and Pt, will also exhibit large no-saturated MR for fields applied in those directions.[20] These MR are positive and linear in high magnetic fields. And, they present obvious anisotropy because of anisotropy of Fermi Surface, which are similar what we observed in *p*-type topological insulator Sb_2Te_3[21]. In addition, no-saturated MR can occur in semiconductors as a consequence of strong electrical disorder, which is related to the carrier mobility but independent of carrier density. They are also positive and have transitions from a quadratic field dependence at low fields to a linear dependence at higher fields. And the high-field MR was found to be linear at all temperatures ranges.[22]

The giant and high-field linear interlayer MR with twofold symmetry of anisotropy in our samples is likely to be related to the configurations of the valence bands. The valence bands of undoped Sb_2Te_3 are multi-valley bands and consist of upper and lower valence bands. Sb_2Te_3 has a non-spherical Fermi surface consisting of six ellipsoids tilted at an angle to the basal plane, where the two valence bands are responsible for conduction.[23] Both valence bands are filled by holes with different mobility, effective mass, and hole concentration in different valleys. The non-saturating linear interlayer MR suggests that holes have open orbits along the Fermi surface, because the MR should saturate at high B if the orbits are closed in high fields.[20] Doping not only increases the density of holes and decreases the mobility of holes, but also increases the additional impurity scattering. The main mechanisms of scattering in *p*-type Sb_2Te_3 are acoustic phonon scattering, impurity scattering, and intra-valley and inter-valley scattering. The giant interlayer MR might come from intra-valley and inter-valley scattering in the upper valence band and impurity scattering from doping induced impurity bands.[21] Furthermore, the upper and lower valence bands in Sb_2Te_3 are anisotropic, with effective mass anisotropy of about 3.8, due to the anisotropy of the ellipsoidal hole pockets.[17] The hole scattering and the relaxation time are anisotropic due to the anisotropy of the ellipsoidal hole pockets. The giant anisotropic interlayer MR might result from the anisotropy of the Fermi surface in *p*-type Bi doped Sb_2Te_3.

5. Conclusions

In conclusion, we measured angle dependent interlayer MR in *p*-type Sb_2Te_3 single crystal and observed giant interlayer MR of up to 400%, which shows strong anisotropy and twofold oscillations. The giant interlayer MR might be due to intra-valley and inter-valley scattering, and the strong anisotropy might result from an anisotropic Fermi surface. The observed giant anisotropic interlayer MR has potential in magneto-electric applications, such as anisotropic magnetic sensors.

Acknowledgements

X. L. Wang thanks the Australian Research Council for supporting this project through a Discovery project.

REFERENCES

1. M. Z. Hasan, and C. L. Kane, *Rev. Mod. Phys.* **82**(4) 3045-3067 (2010).
2. X. L. Qi and S. C. Zhang, *Rev. Mod. Phys.* **83**(4), 1057-1110 (2011).
3. B. A. Bernevig, T. L. Hughes, and S. C. Zhang, *Science* **314**, 1757-1761 (2006).
4. D. Hsieh, D. Qian, L. Wray, Y. Xia, Y. S. Hor, R. J. Cava, and M. Z. Hasan, *Nature* **452**, 970-974 (2008).
5. J. E. Moore, *Nature* **464**, 194-198 (2010).

6. X. L. Wang, S. X. Dou, and C. Zhang, *NPG Asia Mater.* **2**, 31-38 (2010).
7. Y. L. Chen, J. G. Analytis, J. H. Chu, Z. K. Liu, S.K. Mo, X. L. Qi, H. J. Zhang, D. H. Lu, X. Dai, Z. Fang, S. C. Zhang, I. R. Fisher, Z. Hussain, and Z. X. Shen, *Science* **325**(5937), 178-181 (2009).
8. H. J. Zhang, C. X. Liu, X. Liang Qi, X. Dai, Z. Fang, and S. C. Zhang, *Nature Physics* **5**, 438-442 (2009).
9. H. L. Peng, K. J. Lai, D. S. Kong, S. Meister , Y. L. Chen, X. L. Qi, S. C. Zhang, Z. X. Shen, and Y. Cui, *Nat. Mater.* **9**, 225-229 (2010).
10. D. X. Qu, Y. S. Hor, J. Xiong, R. J. Cava, and N. P. Ong, *Science* **329**, 821-824 (2010).
11. A. A. Taskin, and Y. Ando, *Phys. Rev. B* **80**, 085303-085308 (2009).
12. H. Tang, D. Liang, R. L. J. Qiu, and X. P. A. Gao, *ACS Nano*, **5** (9), 7510–7516 (2011).
13. H. Y. Lv, H. J. Liu, L. Pan, Y. W. Wen, X. J. Tan, J. Shi, and X. F. Tang, *Appl. Phys. Lett.* **96**(14), 142101-142103 (2010).
14. D. Kong, Y. L. Chen, J. J. Cha, Q. F. Zhang, J. G. Analytis, K. J. Lai, Z. K Liu, S. S. Hong, K. J. Koski, S. K. Mo, Z. Hussain, I. R. Fisher, Z. X. Shen, and Y. Cui, *Nature Nanotechnology* **6**,705-709 (2011).
15. J. S Zhang, C. Z. Chang, Z. C Zhang, J. Wen, X. Feng, K. Li, M. H. Liu, K. He, L. L. Wang, X. Chen, Q. K. Xue, X. C Ma, and Y. Y. Wang, *Nature Communications* **2**, 574 (2011).
16. A. A. Abrikosov, Phys. Rev. B **85**, 2789 (1998).
17. V. A. Kulbachinskii, Z. M. Dashevskii , M. Inoue, M. Sasaki, , W. X. Gao, P. Lostak, J. Horak, and A. de Visser, *Phys. Rev. B* **52**(15), 10915-10922 (1995).
18. A. A. Abrikosov, *Phys. Rev. B*, **60**(6), 4231-4234 (1999).
19. M. König, S. Wiedmann, C. Brüne, A. Roth, H. Buhmann, L. W. Molenkamp, X. L. Qi, and S. C. Zhang, *Science* **318**(5851), 766-770 (2007).
20. D. Feng, and G. J. Jin, *Introduction to condensed matter physics*, **1**st, (World Scientific Publishing Company, China, 2005) P212
21. E. Fawcett, *Adv. Phys.* **13**, 139 (1964).
22. H. G. Johnson, S. P. Bennett, R. Barua, L. H. Lewis, and D. Heiman, *Phys. Rev. B* **82**(5), 085202-085205 (2010).
23. Y. M. Zuev, J. S. Lee, C. Galloy, H. Park, and P. Kim, *Nano Lett.* **10**, 3037-3040 (2010).

FIGURE CAPTIONS

Figure 1. Interlayer resistivity of *p*-type Sb_2Te_3 as a function of temperatures in zero field. The insets show the measurement schematic diagram.

Figure 2. Interlayer MR as a function of magnetic fields at 0 degree for several temperatures.

Figure 3. Angular dependences of interlayer MR at 2 K in different fields.

Figure 4. Angular dependences of interlayer MR in 13 T at different temperatures.

Figure

Figure 1.

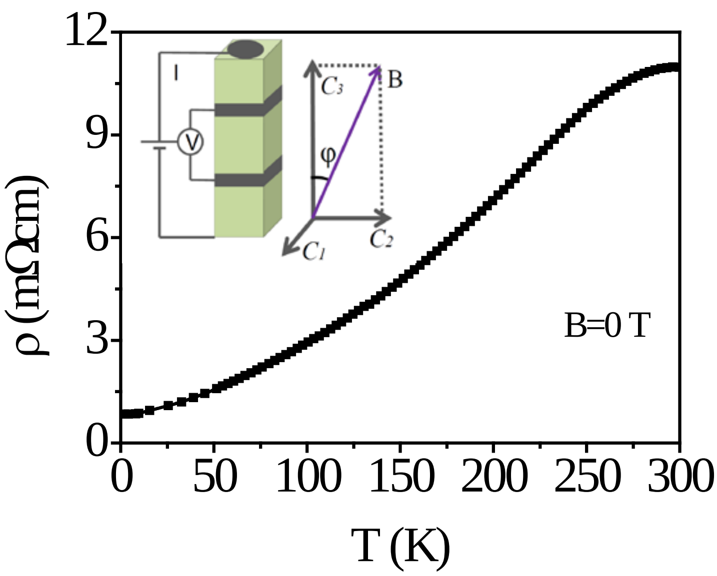

Figure 2.

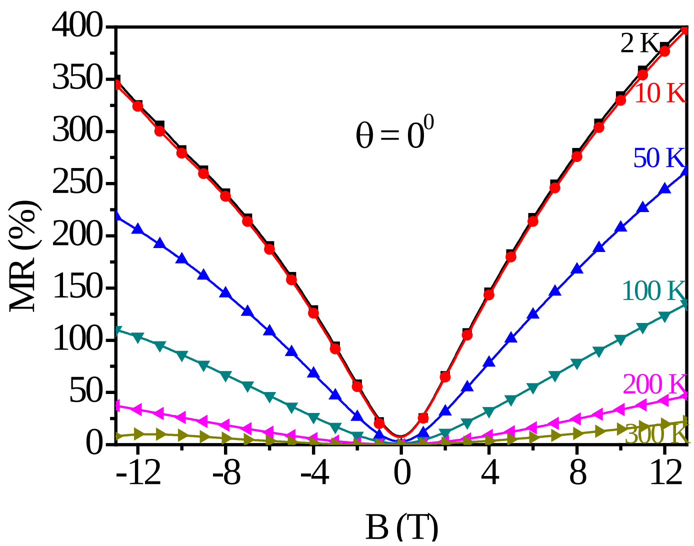

Figure 3.

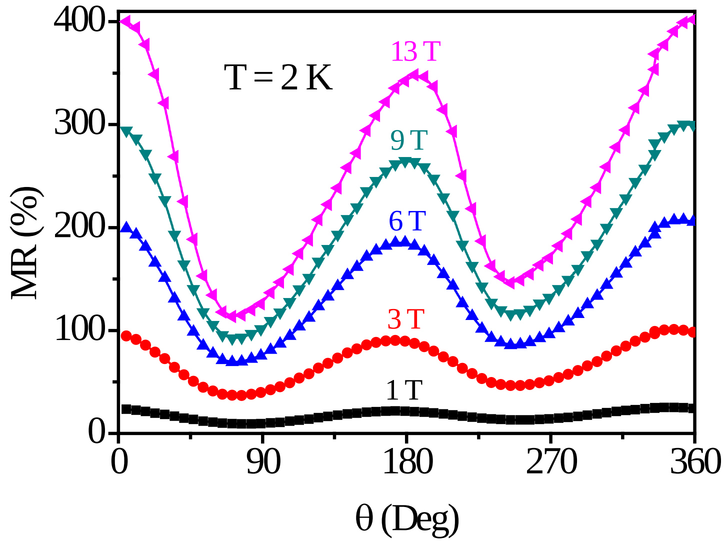
T = 2 K
13 T
9 T
6 T
3 T
1 T
MR (%)
θ (Deg)
0
90
180
270
360
0
100
200
300
400

Figure 4.

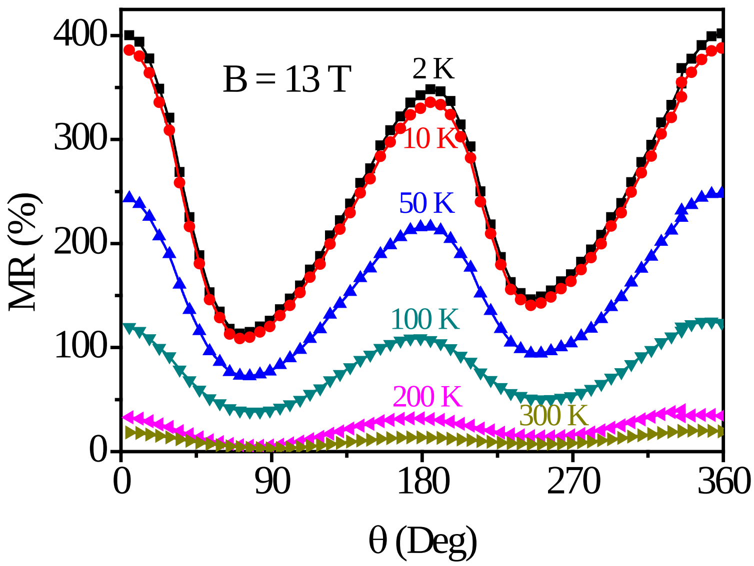
B = 13 T
2 K
10 K
50 K
100 K
200 K
300 K
MR (%)
θ (Deg)
0
90
180
270
360
0
100
200
300
400